ACS OMEGA

http://pubs.acs.org/journal/acsodf

Article

Influence of Henna Extracts on Static and Dynamic Adsorption of Sodium Dodecyl Sulfate and Residual Oil Recovery from Quartz Sand

Mohd Syazwan Mohd Musa, Priveqa Yaashini Gopalan, Nurudeen Yekeen,* and Ahmed Al-Yaseri*

Cite This: *ACS Omega* 2023, 8, 13118−13130

Read Online

ACCESS | Metrics & More | Article Recommendations

ABSTRACT: The application of surfactant flooding for enhanced oil recovery (EOR) promotes hydrocarbon recovery through reduction of oil−water interfacial tension and alteration of oil-wet rock wettability into the water-wet state. Unfortunately, surfactant depletion in porous media, due to surfactant molecule adsorption and retention, adversely affects oil recovery, thus increasing the cost of the surfactant flooding process. Chemical-based materials are normally used as inhibitors or sacrificial agents to minimize surfactant adsorption, but they are quite expensive and not environmentally friendly. Plant-based materials (henna extracts) are far more sustainable because they are obtained from natural sources. However, there is limited research on the application of henna extracts as inhibitors to reduce dynamic adsorption of the surfactant in porous media and improve oil recovery from such media. Thus, henna extracts were introduced as an eco-friendly and low-cost sacrificial agent for minimizing the static and dynamic adsorption of sodium dodecyl sulfate (SDS) onto quartz sand in this study. Results showed that the extent of surfactant adsorption was inversely proportional to the henna extract concentration, and the adsorption of the henna extract onto the quartz surface was a multilayer adsorption that followed the Freundlich isotherm model. Precisely, the henna extract adsorption on quartz sand is in the range of 3.12−4.48 mg/g (for static adsorption) and 5.49−6.73 mg/g (for dynamic adsorption), whereas the SDS adsorption on quartz sand was obtained as 2.11 and 4.79 mg/g at static and dynamic conditions, respectively. In the presence of 8000 mg/L henna extract, SDS static and dynamic adsorption was significantly reduced by 64 and 82%, respectively. At the same conditions, the residual oil recovery increased by 9.2% over normal surfactant flooding. The study suggests that the use of henna extracts as a sacrificial agent during SDS flooding could result in the reduction of static and dynamic adsorption of surfactant molecules on quartz sand, thus promoting hydrocarbon recovery from sandstone formations.

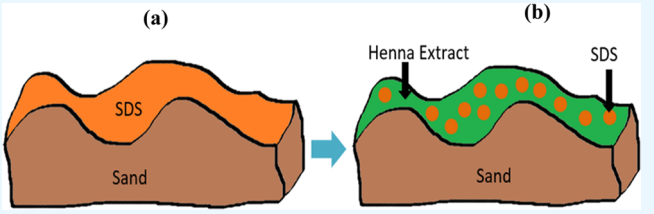

1. INTRODUCTION

Surfactant flooding is a popular enhanced oil recovery (EOR) method that has been proven to be more effective in the mobilization of trapped oil from the hydrocarbon reservoir compared to traditional water flooding.[1] The EOR mechanism of surfactant flooding is oil−water interfacial tension (IFT) reduction and alteration of oil-wet rock wettability into the water-wet state.[2−4] However, the depletion of surfactant molecules through adsorption and retention in the porous media usually increases the cost and decreases the effectiveness and profitability of surfactant flooding.[5]

In general, surfactant adsorption is described as the process by which surfactant molecules migrate from the bulk solution and accumulate at a surface or an interface of a solid or liquid.[6,7] Several forces contribute to the strong affinity between the surfactant molecules and the solid surface, such as micelle-based ion exchange, ion pairing, hydrogen and hydrophobic bonding, pi (π)−electron dispersion, and forces of polar covalent bonding. However, the force of adsorption generally occurs via single-ion interactions.[8]

Likewise, the adsorption isotherms are influenced by several parameters such as the type of salts in the aqueous solution, the surfactant type, the rock morphology and mineralogical composition, the charge on the rock surface, and the pH of the solution.[9,10] Besides surfactant adsorption, reservoir rock heterogeneity as well as the reaction/interaction between the surfactants and reservoir fluids increases the complication of the surfactant system in porous media.[11]

Previous experimental studies have suggested that the most suitable surfactants for sandstone formation are anionic surfactants, whereas cationic surfactants are most promising for carbonate formations, due to the existence of similar surface charges and electrostatic repulsion forces between the

Received: January 18, 2023
Accepted: March 16, 2023
Published: March 28, 2023

surfactant's molecules and the adsorbent surfaces.[12−14] However, at the field scale, it is difficult to determine the most suitable ionic surfactants for EOR applications given the complex heterogeneity of the reservoir, in particular the diverse range of minerals comprising aluminates, carbonates, silicates, and various clays.

Results of the previous research have shown that the adsorption of surfactant molecules on rock surfaces can be minimized through chemical agents, particularly alkali such as sodium hydroxide and sodium carbonate, and through the utilization of sacrificial agent or inhibitor techniques.[15−19] Mechanistically, the sacrificial agents or inhibitors significantly reduced the surfactant adsorption by inhibiting the rock surface and ensured saturation of the active sites of the rock surfaces prior to surfactant injection.[20]

Weston et al.[19] and Bhosle et al.[21] reported that the major mechanism that drives the adsorption process is the formation of admicelles on the solid surface by surfactant molecules. They further emphasized that the inhibition method via sacrificial agents could prevent the formation of these admicelles. However, the experiments of Weston et al.[19] and Bhosle et al.[21] were only limited to dynamic studies and did not provide insights into the impact of sacrificial agents on oil recovery by surfactant flooding. Feng et al.[16] found that the use of alkali lignin as the inhibitor reduced surfactant adsorption on quartz sand, and the rate of surfactant adsorption was inversely proportional to the concentration of alkali lignin. However, the use of alkaline species could result in extreme scaling in the near-wellbore and production systems.[22−24]

Shamsijazeyi et al.[17] examined the influence of polyelectrolytes as inhibitors to reduce the static adsorption of anionic surfactants. They found that 2500 ppm sodium polyacrylate concentration significantly reduced surfactant adsorption on carbonate rock. However, the static adsorption experiment was conducted with a constant concentration of the surfactant. Weston et al.[19] also utilized a polyelectrolyte as an inhibitor in their study and found that the adsorption decreased with increasing polyelectrolyte concentration. However, the silica powder that was used as the adsorbent contained other minerals that could interfere with the adsorption process and outcomes. Moreover, experiments of both Shamsijazeyi et al.[17] and Weston et al.[19] did not assess the EOR potentials of the polyelectrolytes.[25]

Recently, Shye et al.[26] investigated the influence of sodium lignosulfonate as an inhibitor of cationic surfactant adsorption onto kaolinite. They found that the rate of reduction in surfactant adsorption was more significant with increasing sodium lignosulfonate concentration. However, this research was also limited to the static adsorption experiment, and the oil recovery experiment was not conducted to assess the EOR potentials of the sacrificial agent at realistic reservoir conditions. Moreover, the polyelectrolyte and lignosulfonate are natural polymers and lignin derivatives, respectively. The high-molecular weight polymers can still be adsorbed onto the porous media, resulting in reduction in formation permeability and rock formation damage.[27−29]

Generally, chemical-based inhibitors have been the subject of the most previous research; there is still a lack of attention on the potential use of plant-based extracts as inhibitors. The advancement in technology and drive for attainment of decarbonization objectives have placed more emphasis on the economic and environmental implications of chemical-based products. In contrast to chemical constituents, plant-based materials are far more sustainable because of their dependence on fewer natural sources, which reduces environmental pollution and depletion of raw materials in the environment. In addition, the emergence of renewable, low-cost, and eco-friendly plant extracts provides an alternative source to replace toxic chemical inhibitors.

Plant-based materials have been successfully used as corrosion inhibitors in the steel industry and medicine.[30−32] Results of Bhardwaj et al.[30] as well as Miralrio and Vázquez[31] studies showed that the different functional groups of phytochemicals in plants are the key components in the inhibition of steel corrosion. Lorigo and Cairrao[32] also demonstrated that antioxidant molecules in plant extracts could assist the natural antioxidant mechanism in the skin as well as stabilize the UV filters by hindering the accumulation of harmful radicals in the skin.

However, compared to chemical-based materials, the applications of plant-based extracts as inhibitors for reducing surfactant adsorption and improving hydrocarbon recovery from porous media have not been studied in detail. Moreover, most of the previous applications of henna extracts as surfactant molecule adsorption inhibitors have been limited to static experiments. Henna extracts are plant-based water-soluble extracts of the dried flowers, fruit, and leaves of henna, which have recently shown significant inhibition properties in clay−water systems.[33]

This study was motivated by insufficient studies on the dynamic adsorption and EOR potentials of henna extracts as inhibitors/sacrificial agents. Given the economic and environmental benefits of using plant-based extracts as inhibitors to reduce the static and dynamic adsorption of surfactants in porous media, it is essential to conduct more research on the application of henna extracts as inhibitors/sacrificial agents during surfactant flooding.

Consequently, this study was conducted to assess the use of henna extracts as potential inhibitors/sacrificial agents to reduce SDS adsorption on quartz sand through the static and dynamic adsorption study and EOR experiments. The interest and motivation of this study were driven by the limited research on the inhibiting properties of the henna extracts. First, the henna extract and adsorbent sample characterization processes were highlighted. Then, static adsorption and dynamic experiments were conducted and analyzed. Lastly, the oil recovery process in the absence and presence of henna extracts was assessed and discussed.

2. MATERIALS AND METHODS

2.1. Materials. The henna leaves were obtained from henna trees located in Johor Bahru, Malaysia. All chemicals and reagents utilized in this study were of analytical grade. Sodium dodecyl sulfate (SDS) with a purity and molecular weight of 98% and 288.38 g/mol, respectively, was supplied by Fisher Chemical U.K. and applied as the anionic surfactant for the adsorption experiments. Methanol with 99.9% purity was supplied by Across Organics and used as a solvent for the methanolic extraction. Silica sand with a particle size of 150−250 μm[34] was used as the porous media in the cylindrical sandpack. Paraffin oil with a viscosity of 0.8124 g/cm^3 and density of 17.431 cP was used for the displacement experiments. Artificial brine containing 10,000 ppm NaCl (99.8% purity) was supplied by Vchem Malaysia and used in the static adsorption and sandpack experiments. Deionized water (DIW) was used throughout the study.

https://doi.org/10.1021/acsomega.3c00371
ACS Omega 2023, 8, 13118−13130

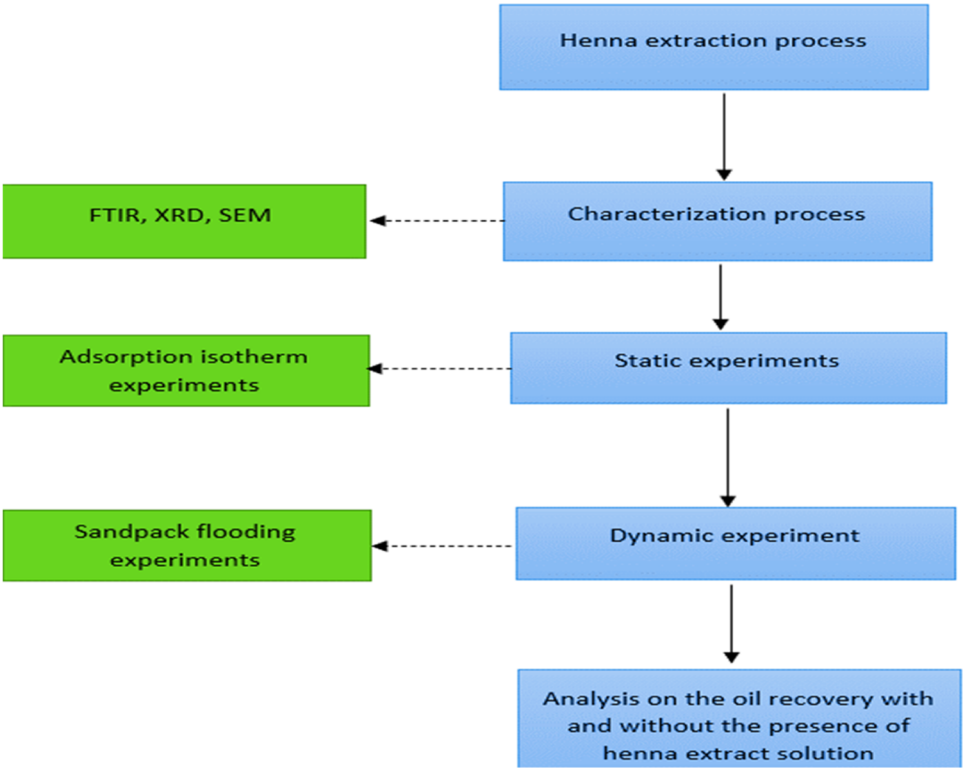

Figure 1. Flowcharts showing the steps of the experiments conducted in this research.

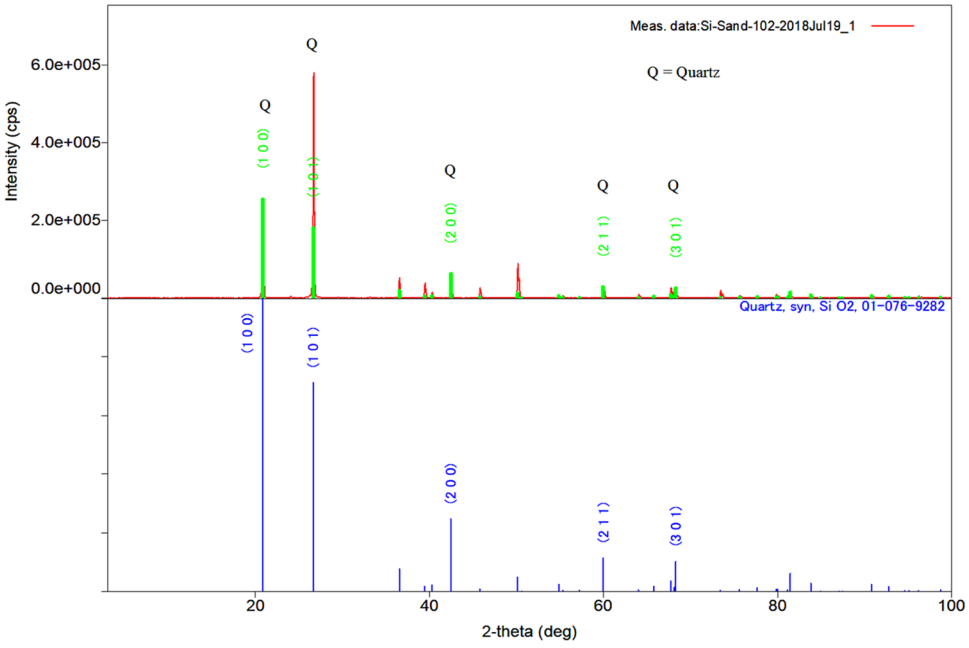

Figure 2. XRD diffractogram of quartz sand.

2.2. Characterizations, Solution Preparation, and CMC Determination. The experimental steps are presented in the form of a flow chart in Figure 1. The attenuated total reflectance (ATR)−Fourier transform infrared (FTIR) spectroscopy analysis was performed with a Perkin Elmer FTIR spectrometer. The spectrometer was also used to detect the functional groups of the henna extract and quartz sand by analyzing the molecules' bond vibrational movement. The spectra were determined with a scan resolution of 2 cm^{-1} in the 650−4000 cm^{-1} range. The FTIR measurements were recorded in the transmittance mode. The spectral profile was then evaluated and compared to the IR absorption table to ascertain the functional groups that are present in the samples.

The mineral composition of the adsorbent sample was identified from the X-ray diffraction (XRD) analysis. This process entails the projection of an X-ray beam onto a sample and analyzing the pattern of X-rays dispersed by the atoms in the substance. The XRD pattern shows a series of peaks that

https://doi.org/10.1021/acsomega.3c00371
ACS Omega 2023, 8, 13118−13130

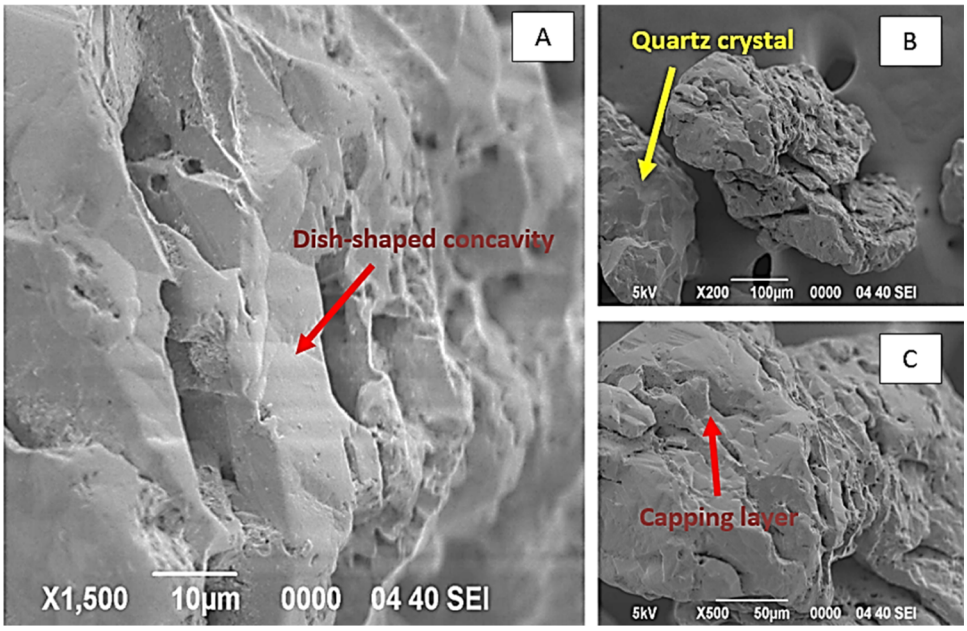

Figure 3. Scanning electron microscopy images of quartz sand showing (a) dish-shaped concavity pattern of quartz, (b) well-preserved quartz crystal surfaces, and (c) existence of a capping layer.

correspond to the scattering of X-rays by the several planes of atoms in the quartz crystal structure. The intensities and angles of these peaks were then measured. Figure 2 depicts the XRD pattern of quartz sand; the diffraction peaks are assigned to quartz sand, which are consistent with the standard data for quartz sand on the ICDD (International Centre for Diffraction Data) card, 01-076-9282. There were no impurity peaks found, and the diffraction peaks had high intensities and sharp peaks, suggesting that the quartz sand is highly crystalline and mainly composed of silicon and oxygen atoms.

The morphology of the quartz sand was assessed from the scanning electron microscopy (SEM) images. The SEM device scanned the quartz sample surface with a focused stream of electrons; secondary electrons are emitted and collected with a detector as the beam interacts with the atoms in the sample. These signals are then used to generate a high-resolution picture of the quartz surface. The SEM images provided vital information on the crystal structure and shape of the mineral. The images of the quartz sand's grain structure are presented in Figure 3 at three magnifications (200×, 500×, and 1500×). The quartz sand was mostly gray to light gray in color, containing fine-textured particles (indicated by the particle sizes, which vary from 150 to 250 μm) to coarse sand and some fine-grained argillaceous varieties with nearly no silt or clay.

The quartz particles have a rounded shape, which denotes the repeated structure and maturity of sedimentary deposition. Higher magnification of a quartz particle reveals a spongy texture and fissures. Figure 3B shows well-preserved quartz crystal surfaces with six surfaces forming a prism. The lower face is a conchoidal fracture face, and transportation pathways can be clearly identified from the rock surface morphologies in Figure 3A. Dish-shaped concavity (an eolian sand index pattern) can also be recognized in Figure 3A. This deep depression can be attributed to mechanical chipping that occurs during very severe sandstorms. The existence of the capping layer can be observed in Figure 3C, signifying deep-burial diagenesis accompanying deposition on the Earth's surface. A thin layer of SiO_2 capping appeared after a specific temperature and pressure threshold has been attained.

Different concentrations of henna extract solution (3000−8000 mg/L) were prepared in standard 250 mL Erlenmeyer flasks. Depending on the desired concentration, the concentrated liquid henna extract was measured and transferred into a conical flask, preceded by the addition of deionized water (DIW). The surfactant solution was prepared similarly to the henna extract solution except that the concentration of the surfactant was fixed at 2000 mg/L throughout the study since the critical micelle concentration (CMC) value of the surfactant was measured as 1800 mg/L.

The concentration at which the surfactant molecules tend to aggregate and generate micelles in substantial amounts is the critical micelle concentration (CMC) of the surfactant.[35] The main objectives of chemical EOR are to reduce the interfacial tension between oil and the displacing fluid and alter rock wettability into the hydrophilic state. The optimum surfactant concentration for attaining the lowest reduction in IFT has been obtained close to the surfactant CMC in previous studies;[36−38] thus, determination of the surfactant CMC is critical for surfactant flooding. The CMC of the SDS was determined using the conductivity method in this study (SevenMulti, Mettler Toledo conductivity meter). The surfactant concentrations were varied from 0.05 to 0.8 wt %, and the conductivity at different concentrations was measured. A graph of conductivity versus surfactant concentration was plotted, and the CMC was taken as the point of inflection on the graph.

2.3. Static Adsorption Experiments. The static adsorption measurements were carried out to evaluate the adsorption performance of the henna extract and surfactant on quartz sand. A wide range of henna extract concentrations (3000−8000 mg/L) were prepared, whereas only one concentration of the SDS surfactant (2000 mg/L) was used. The depletion method was used to compare the adsorption of the henna extract before and after adsorption on quartz sand. Approximately 30 mL of henna extract solution was mixed with 6.0 g of quartz sand, and the mixture was agitated at 180 rpm in a KS 3000 I temperature

https://doi.org/10.1021/acsomega.3c00371
ACS Omega 2023, 8, 13118−13130

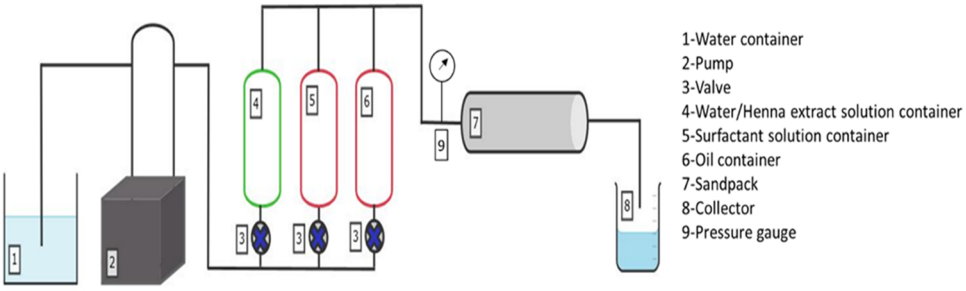

Figure 4. Schematic diagram of the sandpack flooding apparatus.

controller shaker (IKA) for 24 h under atmospheric pressure at 25 °C to achieve the equilibrium state. The solution was then centrifuged at 4000 rpm in a Roto-fix 32A benchtop centrifuge (Hettich Zentrifugen, Germany) for 30 min to collect the buoyant liquid. Ultraviolet−visible spectroscopy (UV-1800 spectrophotometer, Shimadzu, Japan) was used to measure the concentration of the henna extract in the buoyant liquid.

The total adsorption at equilibrium time, q_e (mg/g), was calculated using eq (1), as follows

$$q_e = (C_o - C_e) \times \frac{V}{m} \quad (1)$$

where q_e is the adsorption of the henna extract and surfactant on quartz sand (mg/g), C_o and C_e are the concentrations of the henna extract and surfactant before and after the adsorption experiment, (mg/L) respectively, V is the volume of the henna extract and surfactant solution added in the volumetric flask (L), and m is the total mass of the quartz sand added (g). A similar procedure was repeated for the determination of the surfactant adsorption on quartz sand.

The performance of the henna extract to reduce the surfactant adsorption on quartz sand was determined by filtering out the henna extract-coated quartz sand from the quartz sand solution mixture. The filtered quartz sand, referred to as the pretreated quartz sand, was then mixed with approximately 30 mL of surfactant solution. The mixture was left to reach the equilibrium state for 24 h while recurrently shaken at 180 rpm in the temperature controller shaker. After 24 h, the mixture was centrifuged to obtain the buoyant liquid, which was then analyzed using a UV−vis spectrophotometer. The total adsorption at equilibrium time, q_e (mg/g), was calculated using eq (1).

2.4. Dynamic Adsorption Experiments. The sandpack flooding tests were carried out to assess the dynamic adsorption of the henna extract and SDS on quartz sand. The sandpack was continuously injected with the henna extract solution at a fixed flow rate of 3 mL/min. The effluent sample was collected at the sandpack outlet at specific intervals to analyze the concentration of the henna extract using the UV−vis spectrophotometer. The henna extract concentrations of 3000, 5000, and 8000 mg/L were used in the dynamic adsorption test, which was performed similarly to the surfactant injection test except that the injected surfactant concentration was fixed at 2000 mg/L.

To identify the relationship between the henna extract concentration and the surfactant adsorption on quartz sand, the surfactant was injected in the sandpack flooding at the same flow rate continuously following the injection of the henna extract. The effluent sample was collected at the sandpack outlet at specific time intervals and analyzed for surfactant concentrations using the UV−vis spectrophotometer.

2.5. Enhanced Oil Recovery Experiments. The sandpack flooding experiments were performed to evaluate the effectiveness of the henna extract to reduce surfactant adsorption and increase the residual oil recovery. The increase in oil recovery would indicate the EOR potential of the henna extract as a sacrificial agent. The schematic layout of the sandpack flooding system setup is portrayed in Figure 4.

The flooding experiment was conducted using quartz sand at a fixed temperature of 25 °C. Local sand was filtered in a sieve shaker to prepare the sandpack column with a diameter of 2 cm and length of 25 cm. After sealing the bottom end of the vertically held sandpack with a sieve mesh, artificial brine was added up to the desired level. To eliminate remaining air pockets during the sand pouring process, the level of artificial brine inside the sandpack was kept above the sand. At each step, the sands were tightly packed and devoid of air by shaking the sandpack, while the end of the sandpack was vibrated for 30 min.[39,40]

The flooding experiment was then conducted using artificial brine to evaluate the pore volume of the sandpack for further use in the displacement analysis, which was approximately 91 cm^3 with a porosity of about 28%. The sandpack was saturated with oil at a constant flow rate of 3 mL/min till the water cut dropped to less than 1%. The effluent fluid was collected in a beaker, and the volume of the brine displaced was measured as the volume of oil retained in the sandpack. Once the system was allowed to equilibrate for 24 h, the water flooding test was performed. The residual oil saturation was obtained by injecting the artificial brine into the sandpack at a fixed flow rate of 3 mL/min after the water flooding test.

The water flooding was discontinued when the water cut approached 100%. The effluent fluid was collected in a beaker, and the residual oil saturation was determined by measuring the oil volume in the beaker. Finally, the surfactant slug of 0.75 pore volume (PV) was injected at a fixed flow rate of 3 mL/min, followed by the extended chase water flooding until the water cut reached 100%. The volume of the produced oil was measured according to the material balance approach to determine the residual oil saturation and the oil recovery after the surfactant flooding.

Henna extract flooding with concentrations of 3000, 5000, and 8000 mg/L was performed to evaluate the ability of the henna extract to reduce the surfactant adsorption via sandpack flooding instead of water flooding after the sandpack was saturated with oil. The sandpack was saturated with the henna extract solution at a fixed flow rate of 3 mL/min until the henna extract solutions were 100% at the producer. This step ensures that the henna extract was able to inhibit the quartz sand. This was immediately followed by surfactant flooding and chase water flooding after the henna extract injection was completed.

https://doi.org/10.1021/acsomega.3c00371
ACS Omega 2023, 8, 13118−13130

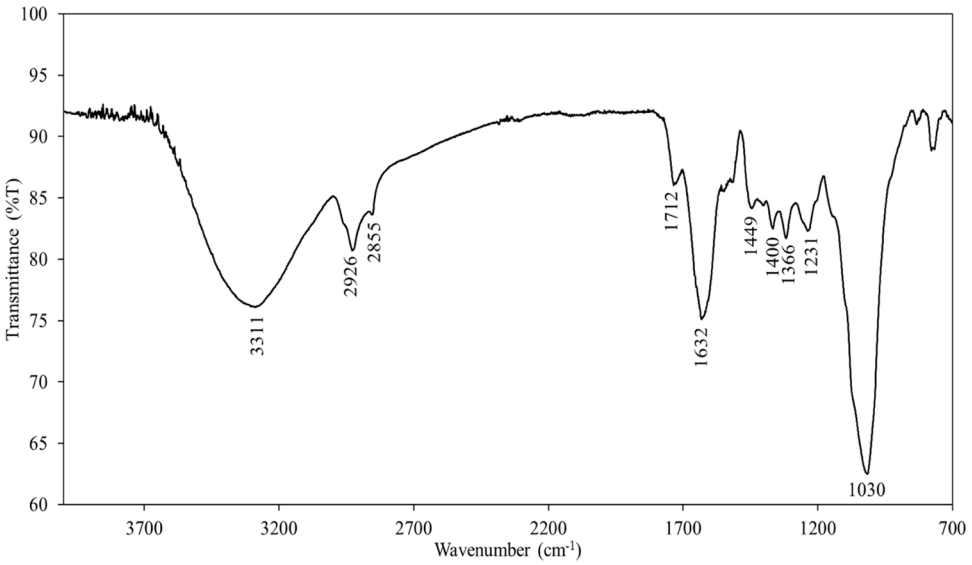

Figure 5. Henna extract FTIR-ATR spectrum.

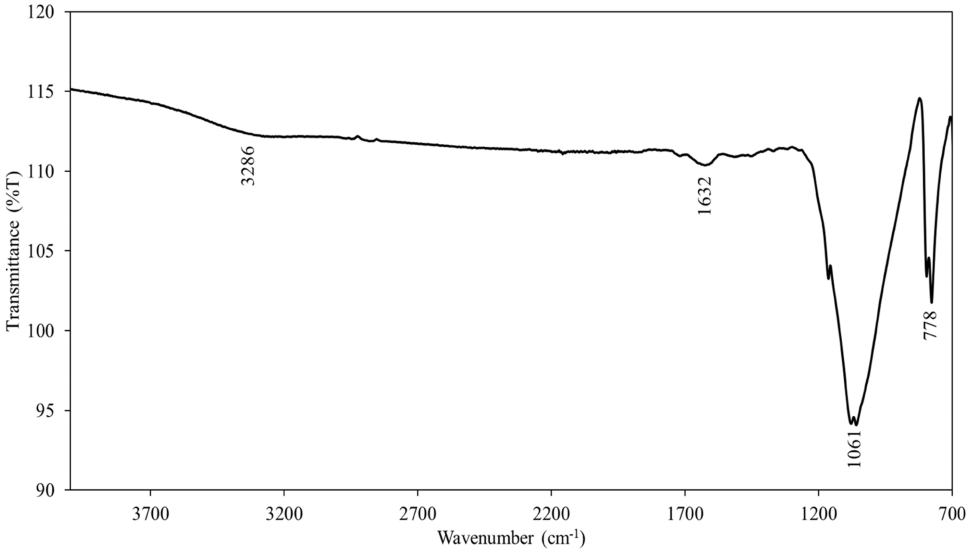

Figure 6. FTIR-ATR spectrum of quartz sand.

3. RESULTS AND DISCUSSION

3.1. FTIR-ATR Spectra of the Henna Extract and Quartz Sand. The henna extract FTIR-ATR spectrum highlighted in Figure 5 shows the presence of an absorption peak at 3311 cm^{-1}, which can be attributed to the O−H (hydroxyl) group vibration. The absorption bands at 2855 cm^{-1} as well as 2926 cm^{-1} result from the vibration of the aliphatic C−H group. Similar functional groups have been identified from the henna extract in the previous studies.[41−45] Other absorption bands at 1632 and 1712 cm^{-1} were due to the presence of the C═O bond. Safie et al.[45] and Zulkifli et al.[46] also observed the same peaks in their study.

The vibration of the C═C group from the aromatic benzene rings resulted in adsorption bands that were observed at 1231, 1366, 1400, and 1449 cm^{-1}. Other researchers have noted similar identical peaks in the henna extract.[41−47] The peak observed at 1030 cm^{-1} can be linked to the vibration of C−O−H of the phenolic group. Similar adsorption bands were observed by Mourão et al.[48] and Saadaoui et al.[49]

The quartz sand infrared spectrum is shown in Figure 6. The infrared bands that were observed at 1632, 3286, and 778 cm^{-1} can be attributed to OH groups from the quartz sand surface, a major composition of SiOH (silanol) groups. Such an adsorption peak has been identified from quartz sand by researchers.[50] The infrared band at 1061 cm^{-1} arises from the vibrations of Si−O−Si and Si−O groups.[51] At ambient temperature, the SiO_2 layer will become saturated in silanol (Si−OH) groups.[52] Moisture (water) certainly exists in the surrounding systems and can readily agglomerate with the O vacancy of the SiO_2 surface to form hydroxyl groups.[53,54]

3.2. FTIR-ATR Analysis of Henna Extract Adsorption onto Quartz Sand. The FTIR spectra of quartz sand before and after henna extract adsorption are shown in Figure 7. The absorption band's intensity of the hydroxyl group in (a) was obvious than before adsorption, which indicates that the henna extract participated in the hydrogen bond between the hydroxyl groups in quartz sand. Since hydrogen is attached to the electronegative oxygen atom (O−H) and because the carbonyl groups (C═O) serve as an electron donor, there is hydrogen

https://doi.org/10.1021/acsomega.3c00371
ACS Omega 2023, 8, 13118−13130

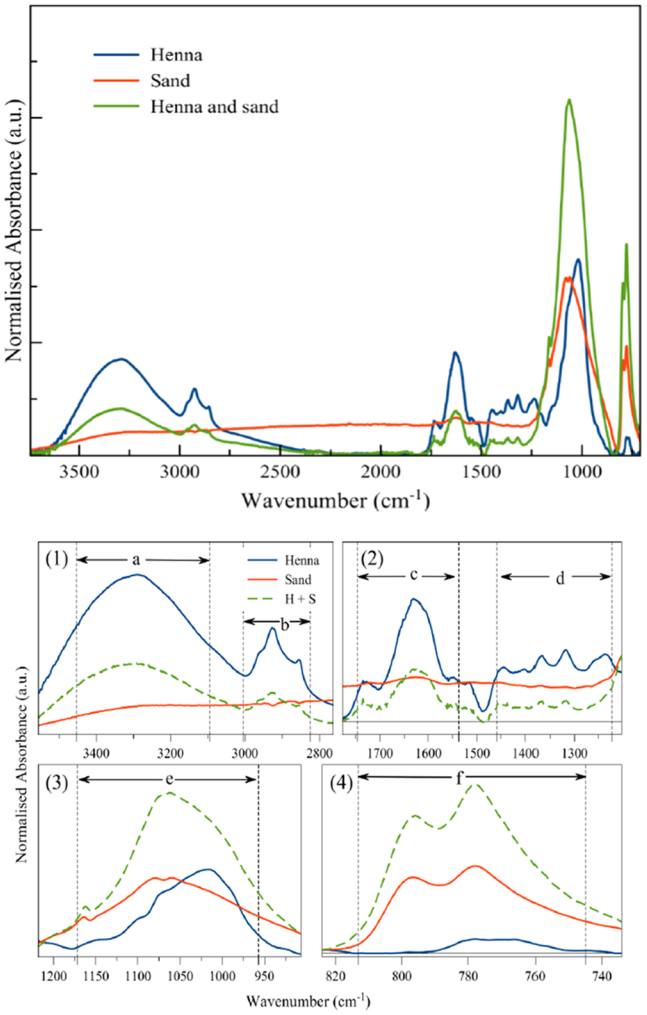

Figure 7. FTIR-ATR spectral analysis of adsorption of the henna extract onto quartz showing (a) hydroxyl group, (b) aliphatic group, (c) carbonyl groups, (d) aromatic rings, (e) phenolic groups, and (f) increased absorption peak due to interactions between the OH group from the quartz sand and henna extract.

bonding occurring between these species. A new absorption band in (b) that belongs to the aliphatic group of the henna extract suggests an interaction with the hydrogen bonds in the quartz sand.

The intensity of the characteristic peaks of carbonyl groups in (c) increased after their adsorption onto the sand, suggesting that the carbonyl groups participated in the adsorption mechanism. The increased intensity of the adsorption band in (d) could be assigned to the aromatic rings, denoting interactions of aromatics with the quartz sand. Increased intensity of the absorption peak of the phenolic groups was observed in (e) with a sharper peak range before the henna extract adsorption, indicating an interaction between the phenolics and quartz. In (f), the absorption peak increased owing to interactions between the OH group from the quartz sand and henna extract.

3.3. Mechanisms of Adsorption of the Henna Extract onto the Solid Surface. The surface of quartz sand comprises mainly Si−O, Si−O−Si, and Si−OH groups. The hydrophilic nature of the hydroxyl group at the quartz sand surface and the hydrophobic nature of the siloxane group (Si−O−Si) prompt the adsorption process. According to Zhuravlev,[55] hydroxyl groups are bound through a valence bond with Si atoms on the quartz sand surface (hydroxyl coverage). Numerous spectral and chemical data clearly confirm the presence of hydroxyl groups on the SiO_2 surface.[55]

The main interactions of Si−OH with the oxygen atom of C═O and with the hydrogen atoms of OH have been attributed to hydrogen bonding.[56] Hydroxyl groups can attach to silicon atoms on sand surfaces through Si−O covalent bonds.[57] The oxygen from the Si−O−Si linkage could develop a hydrogen bond with the hydroxyl groups.[58] Hence, the adsorption mechanism of the henna extract onto the sand surface was governed by hydrogen bonds.

In addition, the benzene ring that is attached to the henna extract can form a cation−π interaction and hydrogen bonding with the hydroxyl groups, further promoting the henna extract adsorption onto the solid surface. Other than hydrogen bonding, the hydrophobic interactions between the siloxane group of quartz sand and the benzene group of the henna extract contributed to the adsorption process.[56] Thus, the mechanisms of adsorption can be identified as hydrogen bonding, hydrophobic interactions, and cation−π interactions.

3.4. Adsorption Isotherm Analysis. Essentially, the adsorption isotherm is a priceless curve that accurately represents the adsorption process and the interactive behavior between solutes and adsorbents. Isotherm assessments can be used to refine the data for the adsorption process planning.[36,37,59,60] In this study, two adsorption isotherm models, namely Langmuir and Freundlich isotherms, were used to analyze the adsorption data. The isothermal adsorption data presented in Figures 8 and 9 were fitted to the Langmuir and

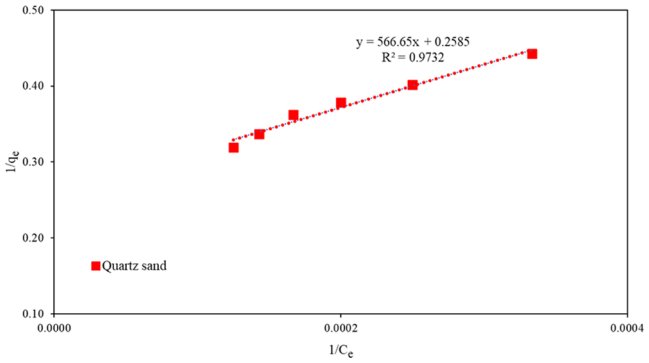

Figure 8. Langmuir isotherm model fit for the adsorption process.

Freundlich isotherm model parameters. These parameters are displayed in Table 1. The results show a high value of R^2 (>0.99) for the Freundlich isotherm, indicating that the adsorption of the henna extract could be clearly expressed using the Freundlich isotherm.

The "n" value indicates the adsorption's favorability; if n equals 1, adsorption is linear. A magnitude of n less than 1 signifies that such an adsorption mechanism is chemical, whereas an n value greater than 1 denotes that the adsorption mechanism is physical.[61,62] The value of n in this study was higher than 1, indicating that henna extract adsorption onto the quartz surface is favorable. Based on the data presented in Table 1, the Freundlich isotherm was the best for representing the adsorption data as proven by the high value of the correlation coefficient, R^2. In addition, the data revealed that the henna extract adsorption demonstrated multilayer adsorption, as shown by the better match of the data to the Freundlich

https://doi.org/10.1021/acsomega.3c00371
ACS Omega 2023, 8, 13118−13130

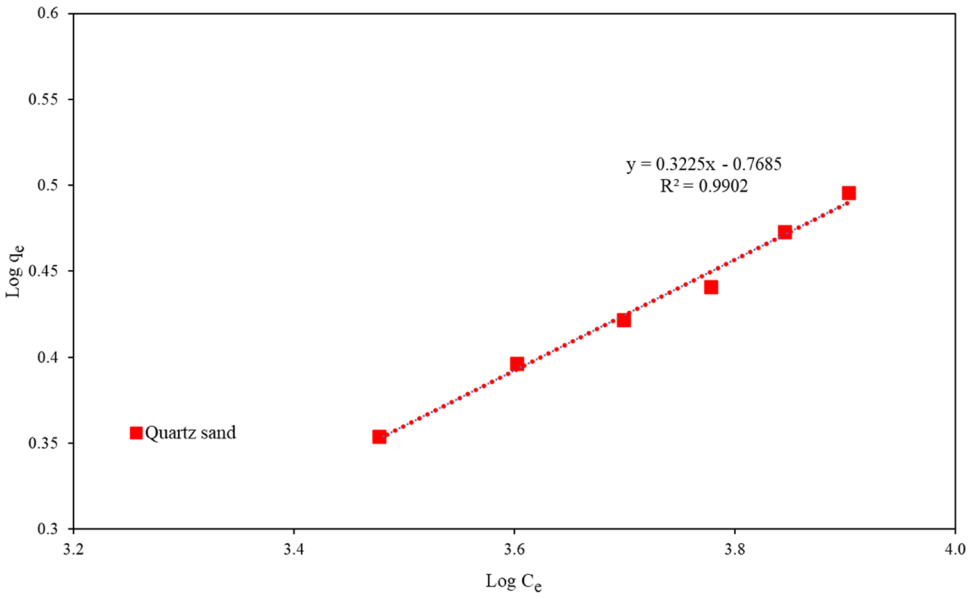

Figure 9. Freundlich isotherm model fit for the adsorption process.

Table 1. Adsorption Isotherm Model Parameters

isotherms	parameters	adsorbent quartz sand
Langmuir	K_L (L/mg)	4.56×10^{-4}
	q_m (mg/g)	3.87
	R^2	0.9732
Freundlich	K_F ((mg/g) (L/mg)$^{1/n}$)	0.17
	n	3.10
	R^2	0.9902

model rather than to the Langmuir model.[63,64] Hence, there was also an adsorbate−adsorbate interaction apart from adsorbate−adsorbent interactions.

3.5. Critical Micelle Concentration of SDS. The plot of conductivity against surfactant concentration is shown in Figure 10. Conductivity increased with increasing surfactant concentrations, but when the surfactant concentration approached a certain amount, the gradient of the graph changed abruptly due to the formation of micelles by the surfactant molecules. Hence, the critical micelle concentration (CMC) of SDS was identified as 1800 mg/L (0.18 wt %). The literature also reported almost similar values of CMC for SDS. Dominguez et al.[65] reported a CMC of SDS of 2300 mg/L, whereas Sanchez-Martin et al.[66] determined the CMC of the SDS surfactant as 2380 mg/L. Furthermore, a CMC value of 2000 mg/L was reported by Yekeen et al.[59] Since the CMC of SDS was determined as 1800, 2000 mg/L SDS concentration was chosen to evaluate the surfactant adsorption performance in the presence of the henna extract in this study.

3.6. Static and Dynamic Adsorption Behavior of the Henna Extract and SDS on Quartz Sand. The static and dynamic adsorption of the henna extract and SDS on quartz sand was plotted against concentration as shown in Figures 11

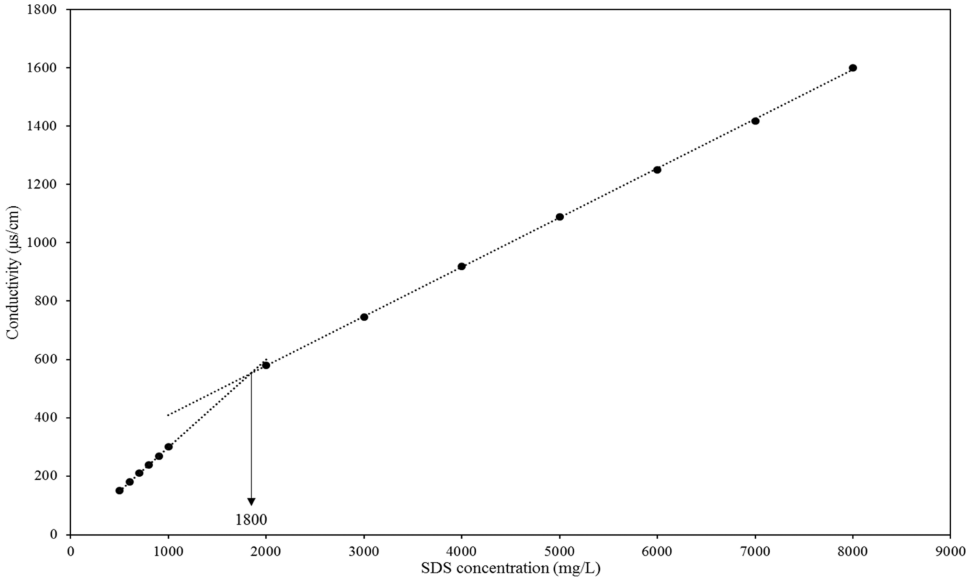

Figure 10. CMC determination of SDS.

https://doi.org/10.1021/acsomega.3c00371
ACS Omega 2023, 8, 13118−13130

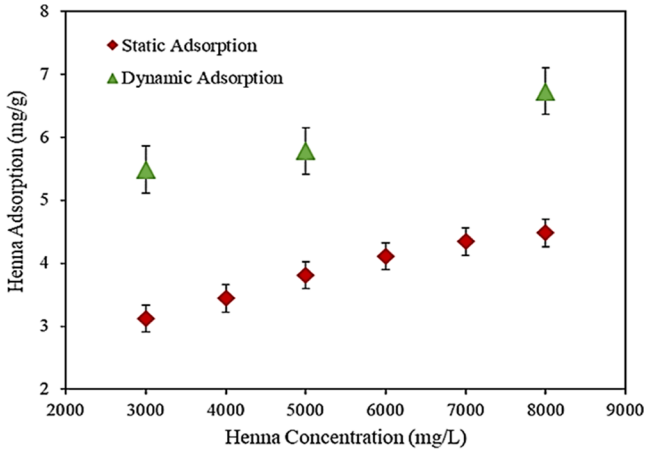

Figure 11. Static and dynamic adsorption of the henna extract on quartz sand.

and 12, respectively. Figure 11 shows that the static adsorption of the henna extract increased (from 3.12 to 4.48 mg/g) with

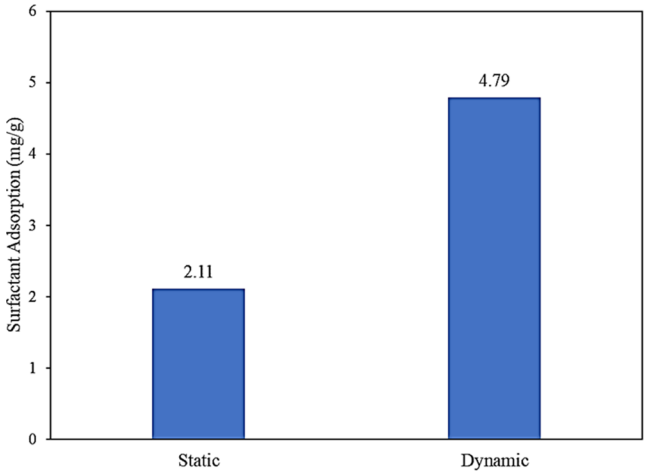

Figure 12. Static and dynamic adsorption of SDS on quartz sand.

increasing concentration from 3000 to 8000 mg/L, whereas for the SDS surfactant, the adsorption was 2.11 mg/g (at a fixed concentration of 2000 mg/g). The findings agreed with result of the previous research, which showed that the adsorption of the adsorbate on the adsorbent increased with increasing concentration of the adsorbate.[17,59,67]

The dynamic adsorption experiments in the sand packs were conducted at different henna extract concentrations (3000, 5000, and 8000 mg/L) and constant SDS concentration (2000 mg/L). Like the static adsorption test, the results indicated that the increase in the concentrations of the henna extract led to the increase in the adsorption on the quartz sand. However, the dynamic adsorption on quartz sand was greater than the static adsorption measurements. The dynamic adsorption of the henna extract was 5.49, 5.78, and 6.73 mg/g for 3000, 5000, and 8000 mg/L of henna extract concentrations, respectively, while the dynamic adsorption of the surfactant was 4.79 mg/g.

The discrepancy between the dynamic and static adsorption results can be attributed to the different methods of conducting the static and dynamic experiments. The static test involved the mixing of quartz sand with a fixed volume of henna extract and surfactant solution to achieve equilibrium. For the dynamic test, the quartz sand inside the sandpack was continuously streamed with the henna extract and surfactant solution with more than 2 PV of the artificial brine. The flooding technique in the dynamic test could have resulted in the adsorption of a greater amount of adsorbed solution on the quartz sand, which affected both the henna extract and surfactant solution.

The adsorption in artificial brine was attributed to the presence of the positively charged cation sodium ions (Na+) in the solution that enhanced the overall electrostatic interactions between the henna extract/SDS and the quartz sand.[2] Belhaj et al.[68] found that adsorption was improved on a negatively charged surface in the presence of salt. A similar trend was obtained by Saxena et al.,[69] which suggested that the presence of salt decreased the electrostatic repulsion between the surface of the adsorbent and the adsorbed henna extract, subsequently promoting the adsorption process.

3.7. Influence of Henna Extracts on Static and Dynamic Adsorption of SDS on Quartz Sand. The static and dynamic adsorption of SDS on quartz was measured at different concentrations of the henna extract (3000, 5000, and 8000 mg/L) to establish the effectiveness of the henna extract as a surfactant inhibitor (Figure 13). The addition of the henna

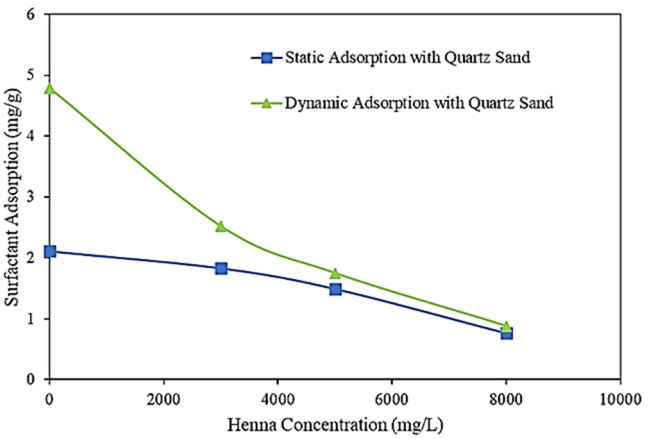

Figure 13. Influence of the henna extract concentration on static and dynamic adsorption of SDS on quartz sand.

extract significantly reduced the amount of the surfactant that was adsorbed on the rock from 2.11 and 4.79 mg/g (without the henna extract) at static test and dynamic conditions to almost 1 mg/g at both conditions. The significant reduction of the surfactant adsorption on quartz sand was consistent with the increase in the henna extract concentration (Figure 13).

The static adsorption of the surfactant decreased from 1.83 to 0.76 mg/g as the concentration of the henna extract was increased from 3000 to 8000 mg/L. The pattern was comparable to that of the dynamic test in which the adsorption of SDS reduced from 4.79 to 2.52 mg/g when 3000 mg/g henna extract was added to the surfactant solutions. The value further dropped to 1.75 and 0.88 mg/g when the concentration of the henna extract was increased to 5000 and 8000 mg/g, respectively.

A maximum of 64% reduction in static adsorption and 82% reduction in dynamic adsorption were observed when 8000 mg/L henna extract was introduced into the SDS solutions. These results suggest that the henna extract was retained in the active sites of the rock, wherein they were able to block the quartz sand surface and prevent interactions between the solid surface and

https://doi.org/10.1021/acsomega.3c00371
ACS Omega 2023, 8, 13118−13130

Table 2. Detail of Sandpack Flooding Experiments

flooding experiment no.	porosity (%)	permeability (mD)	initial oil saturation (%)	henna extract concentration (mg/L)	water flooding/henna extract flooding oil recovery (%)	slug size (PV)	surfactant flooding oil recovery (%)	total oil recovery (%)
1	28.02	3291	84.3	0	22.1	0.75	6	28.1
2	27.98	3276	82.5	3000	25.1	0.75	7.1	32.2
3	28.05	3288	82.8	5000	25.5	0.75	11.2	36.7
4	28.11	3293	83.6	8000	25.7	0.75	11.6	37.3

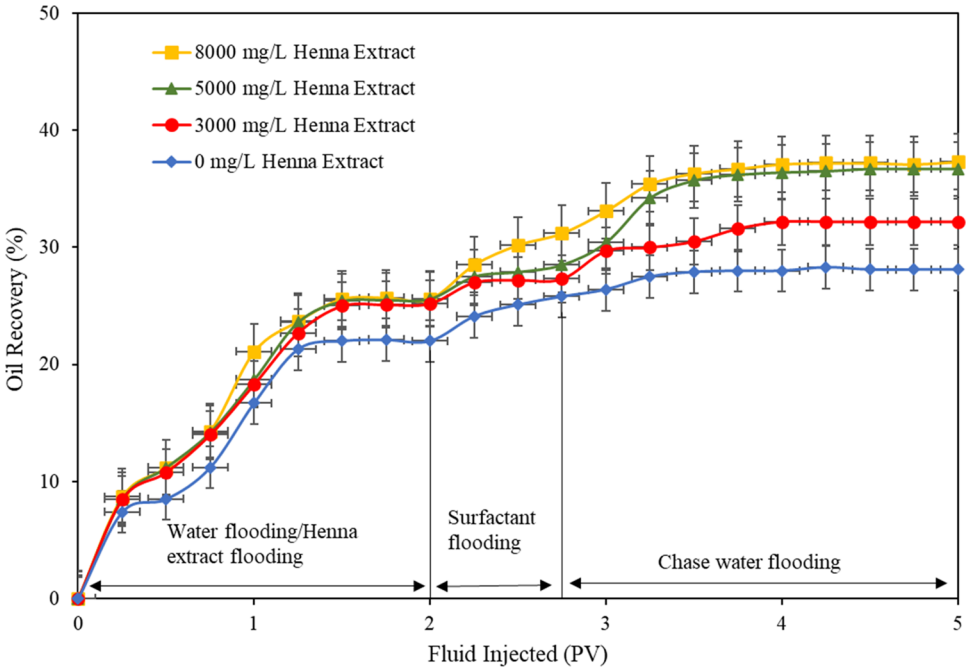

Figure 14. Oil recovery profiles at various henna extract concentrations.

the surfactant molecules, thus decreasing the adsorption of the SDS surfactant on the quartz surface.

3.8. Improved Oil Recovery with Henna Extract Solutions. The sandpack flooding experiments were conducted to evaluate the capability of henna extract solutions to improve oil recovery. Results are presented in Table 2 for different concentrations of henna extract solutions (3000, 5000, and 8000 mg/g). Based on the oil recovery profiles shown in Figure 14, a complete dynamic adsorption process was recorded for the henna extract on the sandpack.

The henna extract flooding reached saturation once the volume injected was beyond 1.25 PV, indicating that all the henna extract solution managed to exit from the sandpack. Furthermore, the water flooding reached equilibrium as the injection volume reached 5 PV. Eventually, a clean sandpack was observed after the water flooding test, indicating the displacement of most of the trapped oil. Under normal surfactant flooding, the oil recovery was 28.1%. The presence of 3000 mg/L henna extract increased the total oil recovery to 32.2%.

Despite the significant increase of oil recovery with the increase in the henna extract concentration, the trend almost reached a plateau when 8000 mg/L henna extract was injected, suggesting that there would be no significant difference if the concentration of the injected henna extract exceeds 8000 mg/L. However, further analysis should be performed in future studies to confirm this assumption.

Meanwhile, the maximum residual oil recovery was recorded with 8000 mg/L henna extract concentration as 37.3%. The oil displacement from the porous media during normal surfactant flooding was smaller because the available surfactant molecules that can lower the oil–water interfacial tension reduced due to surfactant adsorption. The presence of the henna extract increased the oil recovery by 9.2% over the normal surfactant flooding because the presence of the henna extract in surfactant solutions reduced the adsorption of the surfactant on the sand surface; this process was crucial to improve the performance of the surfactant flooding.

The oil recovery significantly increased with increasing henna extract concentration until 8000 mg/L. Generally, the sandpack flooding experiment data confirmed the potential use of henna extracts as an efficient sacrificial agent as previously observed from the static and dynamic adsorption experiments. The henna extract inhibitor obstructed the surface of the quartz sand from adsorbing the available SDS molecules and hence improved the overall oil recovery process. Based on these properties, henna extracts are recommended as sustainable and environmentally friendly plant-based inhibitors.[70]

4. CONCLUSIONS AND RECOMMENDATION

This study was conducted to assess the feasibility of reducing the static and dynamic adsorption of the sodium dodecyl sulfate surfactant on quartz sand using henna extracts as an inhibitor. The enhanced oil recovery potential of the henna extract was also investigated through sandpack flooding experiments. The following are the main conclusions from the study.

https://doi.org/10.1021/acsomega.3c00371
ACS Omega 2023, 8, 13118−13130

(1) The surfactant adsorption was found to exhibit an inversely proportional relationship to the henna extract concentration, suggesting that the contact between the surfactant molecules and quartz sand surface was reduced as a higher concentration of the henna extract occupied the surface of quartz sand, consequently minimizing surfactant adsorption on the quartz sand surface.

(2) The adsorption of the henna extract onto the quartz surface was favorable, and the value of regression coefficients (R^2) was higher when the adsorption data were fitted with the Freundlich isotherm model compared to the Langmuir model, indicating that the adsorption process is multilayer adsorption that could be clearly described using the Freundlich isotherm model.

(3) The study demonstrated that the henna extract is a promising inhibitor that could be effectively utilized to reduce SDS surfactant adsorption and achieve a greater oil recovery through henna extract adsorption on active sites of the quartz sand surface via hydrogen bonding, hydrophobic interactions, and cation−π interactions.

(4) The dynamic adsorption was generally higher than static adsorption; however, the presence of 8000 mg/L henna extract in surfactant solutions resulted in 64 and 82% reduction in static and dynamic adsorption, respectively, and increased the oil recovery by 9.2% over the normal surfactant flooding.

(5) Results of this study suggest that the adsorption phenomenon should not be inferred from static adsorption only, but static adsorption results should be complemented with dynamic adsorption and sandpack/core flooding experiments.

This study provides insights into the feasibility of using henna extracts as a sacrificial agent and inhibitor to reduce the static as well as dynamic adsorption of SDS molecules on quartz sand. However, the static adsorption would be largely influenced by the surface area (the size of the smashed powders). Thus, the influence of the surface area should be considered in future studies and the dynamic adsorption tests should be conducted using reservoir/outcrop rocks for more informative assessment. In this study, only NaCl was used to assess the effects of salinity on the adsorption characteristics of the henna extract and surfactants. High positive ions in reservoirs, such as Ca^{2+} and Mg^{2+}, also have great influences on the adsorption of surfactants; thus, the role of divalent and trivalent cations salts as well as the pH in the adsorption of SDS and henna extracts onto the quartz sand needs to be investigated further.

AUTHOR INFORMATION

Corresponding Authors

Nurudeen Yekeen − *Department of Petroleum Engineering, Universiti Teknologi PETRONAS, Seri Iskandar 32610 Perak, Malaysia; School of Engineering, Edith Cowan University, Joondalup 6027 WA, Australia;* orcid.org/0000-0001-6738-7893; Email: peteryekeen@yahoo.com

Ahmed Al-Yaseri − *Center of Integrative Petroleum Research (CIPR), College of Petroleum Engineering and Geoscience, King Fahd University of Petroleum and Minerals, Dhahran 31261, Saudi Arabia;* orcid.org/0000-0001-9094-1258; Email: ahmed.yaseri@kfupm.edu.sa

Authors

Mohd Syazwan Mohd Musa − *Faculty of Engineering, Universiti Malaysia Sabah, 88400 Kota Kinabalu, Sabah, Malaysia*

Priveqa Yaashini Gopalan − *Faculty of Engineering, Universiti Malaysia Sabah, 88400 Kota Kinabalu, Sabah, Malaysia*

Complete contact information is available at: https://pubs.acs.org/10.1021/acsomega.3c00371

Notes

The authors declare no competing financial interest.

NOMENCLATURE

CMC - critical micelle concentration
DIW - deionized water
FTIR-ATR - Fourier transform infrared−attenuated total reflectance
SDS - sodium dodecyl sulfate
SEM - scanning electron microscopy
EOR - enhanced oil recovery
UV−vis - ultraviolet visible
XRD - X-ray diffraction
PV - pore volume
NaCl - sodium chloride

REFERENCES

(1) Jha, N. K.; Lebedev, M.; Iglauer, S.; Ali, M.; Roshan, H.; Barifcani, A.; Sangwai, J. S.; Sarmadivaleh, M. Pore scale investigation of low salinity surfactant nanofluid injection into oil saturated sandstone via X-ray micro-tomography. *J. Colloid Interface Sci.* **2020**, *562*, 370−380.

(2) Druetta, P.; Picchioni, F. Surfactant-polymer interactions in a combined enhanced oil recovery flooding. *Energies* **2020**, *13*, 6520.

(3) Al-Anssari, S.; Arain, Z.-U.-A.; Barifcani, A.; Keshavarz, A.; Ali, M.; Iglauer, S. In *Influence of Pressure and Temperature on CO2-Nanofluid Interfacial Tension: Implication for Enhanced Oil Recovery and Carbon Geosequestration*; Abu Dhabi International Petroleum Exhibition & Conference; OnePetro, 2018, DOI: 10.2118/192964-MS.

(4) Nazarahari, M. J.; Manshad, A. K.; Ali, M.; Ali, J. A.; Shafiei, A.; Sajadi, S. M.; Moradi, S.; Iglauer, S.; Keshavarz, A. Impact of a novel biosynthesized nanocomposite (SiO_2@ Montmorilant@ Xanthan) on wettability shift and interfacial tension: Applications for enhanced oil recovery. *Fuel* **2021**, *298*, No. 120773.

(5) Hanamertani, A. S.; Pilus, R. M.; Idris, A. K.; Irawan, S.; Tan, I. M. Ionic liquids as a potential additive for reducing surfactant adsorption onto crushed Berea sandstone. *J. Pet. Sci. Eng.* **2018**, *162*, 480−490.

(6) Lu, J.; Liyanage, P. J.; Solairaj, S.; Adkins, S.; Arachchilage, G. P.; Kim, D. H.; Britton, C.; Weerasooriya, U.; Pope, G. A. New surfactant developments for chemical enhanced oil recovery. *J. Pet. Sci. Eng.* **2014**, *120*, 94−101.

(7) Raffa, P.; Broekhuis, A. A.; Picchioni, F. Polymeric surfactants for enhanced oil recovery: A review. *J. Pet. Sci. Eng.* **2016**, *145*, 723−733.

(8) Tamjidi, S.; Moghadas, B. K.; Esmaeili, H.; Khoo, F. S.; Gholami, G.; Ghasemi, M. Improving the surface properties of adsorbents by surfactants and their role in the removal of toxic metals from wastewater: A review study. *Process Saf. Environ. Prot.* **2021**, *148*, 775−795.

(9) Ahmadi, M. A.; Shadizadeh, S. R. Spotlight on the new natural surfactant flooding in carbonate rock samples in low salinity condition. *Sci. Rep.* **2018**, *8*, No. 10985.

(10) Nandwani, S. K.; Chakraborty, M.; Gupta, S. Adsorption of surface active ionic liquids on different rock types under high salinity conditions. *Sci. Rep.* **2019**, *9*, No. 14760.

(11) Machale, J.; Majumder, S. K.; Ghosh, P.; Sen, T. K.; Saeedi, A. Impact of mineralogy, salinity, and temperature on the adsorption characteristics of a novel natural surfactant for enhanced oil recovery. *Chem Eng. Commun.* **2022**, *209*, 143−157.

(12) Ishiguro, M.; Koopal, L. K. Surfactant adsorption to soil components and soils. *Adv. Colloid Interface Sci.* **2016**, *231*, 59−102.
(13) Massarweh, O.; Abushaikha, A. S. The use of surfactants in enhanced oil recovery: A review of recent advances. *Energy Rep.* **2020**, *6*, 3150−3178.
(14) Haghighi, O. M.; Zargar, G.; Khaksar Manshad, A.; Ali, M.; Takassi, M. A.; Ali, J. A.; Keshavarz, A. Effect of environment-friendly non-ionic surfactant on interfacial tension reduction and wettability alteration; implications for enhanced oil recovery. *Energies* **2020**, *13*, 3988.
(15) Budhathoki, M.; Barnee, S. H. R.; Shiau, B.-J.; Harwell, J. H. Improved oil recovery by reducing surfactant adsorption with polyelectrolyte in high saline brine. *Colloids Surf., A* **2016**, *498*, 66−73.
(16) Feng, A.; Zhang, G.; Ge, J.; Jiang, P.; Pei, H.; Zhang, J.; Li, R. *Study of Surfactant-Polymer Flooding in Heavy Oil Reservoirs*, SPE Heavy Oil Conference Canada; OnePetro, 2012 DOI: 10.2118/157621-MS.
(17) ShamsiJazeyi, H.; Verduzco, R.; Hirasaki, G. J. Reducing adsorption of anionic surfactant for enhanced oil recovery: Part II. Applied aspects. *Colloids Surf., A* **2014**, *453*, 168−175.
(18) Wang, J.; Han, M.; Fuseni, A. B.; Cao, D. In *Surfactant Adsorption in Surfactant-Polymer Flooding for Carbonate Reservoirs*, SPE Middle East Oil & Gas Show and Conference; OnePetro, 2015, https://doi.org/SPE-172700-MS.
(19) Weston, J. S.; Harwell, J. H.; Shiau, B. J.; Kabir, M. Disrupting admicelle formation and preventing surfactant adsorption on metal oxide surfaces using sacrificial polyelectrolytes. *Langmuir* **2014**, *30*, 6384−6388.
(20) Wu, Y.; Chen, W.; Dai, C.; Huang, Y.; Li, H.; Zhao, M.; He, L.; Jiao, B. Reducing surfactant adsorption on rock by silica nanoparticles for enhanced oil recovery. *J. Pet. Sci. Eng.* **2017**, *153*, 283−287.
(21) Bhosle, M. R.; Joshi, S. A.; Bondle, G. M. An efficient contemporary multicomponent synthesis for the facile access to coumarin-fused new thiazolyl chromeno [4, 3-b] quinolones in aqueous micellar medium. *J. Heterocycl. Chem.* **2020**, *57*, 456−468.
(22) Chen, L.; Zhang, G.; Ge, J.; Jiang, P.; Tang, J.; Liu, Y. Research of the heavy oil displacement mechanism by using alkaline/surfactant flooding system. *Colloids Surf., A* **2013**, *434*, 63−71.
(23) Tay, A.; Oukhemanou, F.; Wartenberg, N.; Moreau, P.; Guillon, V.; Delbos, A.; Tabary, R. In *Adsorption Inhibitors: A New Route to Mitigate Adsorption in Chemical Enhanced Oil Recovery*, SPE Asia Pacific Enhanced Oil Recovery Conference; OnePetro, 2015, DOI: 10.2118/174603-MS.
(24) Zhang, G.; Yu, J.; Du, C.; Lee, R. In *Formulation of Surfactants for Very Low/High Salinity Surfactant Flooding without Alkali*, SPE International Symposium on Oilfield Chemistry; OnePetro, 2015, DOI: 10.2118/173738-MS.
(25) ShamsiJazeyi, H.; Verduzco, R.; Hirasaki, G. J. Reducing adsorption of anionic surfactant for enhanced oil recovery: Part I. Competitive adsorption mechanism. *Colloids Surf., A* **2014**, *453*, 162−167.
(26) Chong, A. S.; Manan, M. A.; Idris, A. K. Sodium lignosulfonate as sacrificial agent and effectiveness in reducing CTAB cationic adsorption onto kaolinite. *J. King Saud Univ., Eng. Sci.* **2021**, *33*, 539−546.
(27) Xiao, J.; Qiao, G. Understanding the problems and challenges of polymer flooding technique. *Oil Gas Res.* **2017**, *03*, 2472−2518.
(28) Kumar, R.; He, J.; Bataweel, M.; Nasr-El-Din, H. New insights on the effect of oil saturation on the optimal acid-injection rate in carbonate acidizing. *SPE J.* **2018**, *23*, 969−984.
(29) Mohamed, I.; He, J.; Nasr-El-Din, H. A. Effect of Brine Composition on CO_2/Limestone Rock Interactions during CO_2 Sequestration. *J. Pet. Sci. Res.* **2013**, *2*, 14−26.
(30) Bhardwaj, N.; Sharma, P.; Kumar, V. Phytochemicals as steel corrosion inhibitor: an insight into mechanism. *Corros. Rev.* **2021**, *39*, 27−41.
(31) Miralrio, A.; Espinoza Vázquez, A. Plant extracts as green corrosion inhibitors for different metal surfaces and corrosive media: a review. *Processes* **2020**, *8*, 942.
(32) Lorigo, M.; Cairrao, E. Antioxidants as stabilizers of UV filters: An example for the UV-B filter octylmethoxycinnamate. *Biomed. Dermatol.* **2019**, *3*, No. 11.
(33) Aghajafari, A. H.; Shadizadeh, S. R.; Shahbazi, K.; Tabandehjou, H. Kinetic modeling of cement slurry synthesized with Henna extract in oil well acidizing treatments. *Petroleum* **2016**, *2*, 196−207.
(34) Romanova, U.; Gillespie, G.; Sladic, J.; Ma, T.; Solvoll, T.; Andrews, J. A Comparative Study of Wire Wrapped Screens vs. Slotted Liners for Steam Assisted Gravity Drainage Operations. *World Heavy Oil Congr.* **2014**, 5−7.
(35) Yekeen, N.; Salampessy, S. N.; Bakar, A. H. A.; Ali, M.; Okunade, O. A.; Musa, S. A.; Bavoh, C. B. Synthesis and pore-scale visualization studies of enhanced oil recovery mechanisms of rice straw silica nanoparticles. *Geoenergy Sci. Eng.* **2023**, *221*, No. 111292.
(36) Yekeen, N.; Al-Yaseri, A.; Idris, A. K.; Khan, J. A. Comparative effect of zirconium oxide (ZrO_2) and silicon dioxide (SiO_2) nanoparticles on the adsorption properties of surfactant-rock system: Equilibrium and thermodynamic analysis. *J. Pet. Sci. Eng.* **2021**, *205*, No. 108817.
(37) Okunade, O. A.; Yekeen, N.; Padmanabhan, E.; Al-Yaseri, A.; Idris, A. K.; Khan, J. A. Shale core wettability alteration, foam and emulsion stabilization by surfactant: Impact of surfactant concentration, rock surface roughness and nanoparticles. *J. Pet. Sci. Eng.* **2021**, *207*, No. 109139.
(38) Afolabi, F.; Mahmood, S. M.; Yekeen, N.; Akbari, S.; Sharifigaliuk, H. Polymeric surfactants for enhanced oil recovery: A review of recent progress. *J. Pet. Sci. Eng.* **2022**, *208*, No. 109358.
(39) Fu, L.; Zhang, G.; Ge, J.; Liao, K.; Pei, H.; Jiang, P.; Li, X. Study on organic alkali-surfactant-polymer flooding for enhanced ordinary heavy oil recovery. *Colloids Surf., A* **2016**, *508*, 230−239.
(40) Gong, H.; Li, Y.; Dong, M.; Ma, S.; Liu, W. Effect of wettability alteration on enhanced heavy oil recovery by alkaline flooding. *Colloids Surf., A* **2016**, *488*, 28−35.
(41) Rajendran, S.; Agasta, M.; Devi, R. B.; Devi, B. S.; Rajam, K.; Jeyasundari, J. Corrosion inhibition by an aqueous extract of Henna leaves (*Lawsonia inermis* L). *Zašt. Mater.* **2009**, *50*, 77−84.
(42) Nik, W. W.; Zulkifli, F.; Sulaiman, O.; Samo, K.; Rosliza, R. In *Study of Henna (Lawsonia inermis) as Natural Corrosion Inhibitor for Aluminum Alloy in Seawater*, IOP Conference Series: Materials Science and Engineering; IOP Publishing, 2012, 012043, Vol. 36, DOI: 10.1088/1757-899X/36/1/012043.
(43) Mounaouer, B.; Wali, A.; Fourti, O.; Hassen, A. Henna wood as an adsorptive material for bentazon. *Afr. J. Biotechnol.* **2014**, *13*, 3597−3606.
(44) Ebrahimi, I.; Parvinzadeh Gashti, M. Extraction of polyphenolic dyes from henna, pomegranate rind, and Pterocarya fraxinifolia for nylon 6 dyeing. *Color. Technol.* **2016**, *132*, 162−176.
(45) Safie, N. E.; Ludin, N. A.; Su'ait, M. S.; Hamid, N. H.; Sepeai, S.; Ibrahim, M. A.; Teridi, M. A. M. Preliminary study of natural pigments photochemical properties of curcuma longa l. and lawsonia inermis l. as tio 2 photoelectrode sensitizer. *Malaysian J. Anal. Sci.* **2015**, *19*, 1243−1249.
(46) Zulkifli, F.; Ali, N. A.; Yusof, M. S. M.; Khairul, W. M.; Rahamathullah, R.; Isa, M. I. N.; Wan Nik, W. B. The effect of concentration of Lawsonia inermis as a corrosion inhibitor for aluminum alloy in seawater. *Adv. Phys. Chem.* **2017**, *2017*, No. 8521623.
(47) Hamdy, A.; El-Gendy, N. S. Thermodynamic, adsorption and electrochemical studies for corrosion inhibition of carbon steel by henna extract in acid medium. *Egypt. J. Pet.* **2013**, *22*, 17−25.
(48) Mourão, P.; Laginhas, C.; Custódio, F.; Nabais, J. V.; Carrott, P.; Carrott, M. R. Influence of oxidation process on the adsorption capacity of activated carbons from lignocellulosic precursors. *Fuel Process. Technol.* **2011**, *92*, 241−246.
(49) Saadaoui, S.; Youssef, M. A. B.; Karoui, M. B.; Gharbi, R.; Smecca, E.; Strano, V.; Mirabella, S.; Alberti, A.; Puglisi, R. A. Performance of natural-dye-sensitized solar cells by ZnO nanorod and nanowall enhanced photoelectrodes. *Beilstein J. Nanotechnol.* **2017**, *8*, 287−295.

(50) Akl, M. A.; Aly, H. F.; Soliman, H. M. A.; Abd ElRahman, A. M. E.; Abd-Elhamid, A. I. Preparation and characterization of silica nanoparticles by wet mechanical attrition of white and yellow sand. *J. Nanomed. Nanotechnol.* **2013**, *04*, No. 1000183.
(51) Söderholm, K.-J. M.; Shang, S.-W. Molecular orientation of silane at the surface of colloidal silica. *J. Dent. Res.* **1993**, *72*, 1050−1054.
(52) Wu, X.; Sacher, E.; Meunier, M. The effects of hydrogen bonds on the adhesion of inorganic oxide particles on hydrophilic silicon surfaces. *J. Appl. Phys.* **1999**, *86*, 1744−1748.
(53) Chang, J.-G.; Chen, H.-T.; Ju, S.-P.; Chen, H.-L.; Hwang, C.-C. Role of Hydroxyl Groups in the NH x (x = 1 − 3) Adsorption on the TiO2 Anatase (101) Surface Determined by a First-Principles Study. *Langmuir* **2010**, *26*, 4813−4821.
(54) Tilocca, A.; Selloni, A. Structure and reactivity of water layers on defect-free and defective anatase TiO_2 (101) surfaces. *J. Phys. Chem. B* **2004**, *108*, 4743−4751.
(55) Zhuravlev, L. The surface chemistry of amorphous silica. Zhuravlev model. *Colloids Surf., A* **2000**, *173*, 1−38.
(56) Parida, S. K.; Dash, S.; Patel, S.; Mishra, B. Adsorption of organic molecules on silica surface. *Adv. Colloid Interface Sci.* **2006**, *121*, 77−110.
(57) Li, A.; Liu, Y.; Szlufarska, I. Effects of interfacial bonding on friction and wear at silica/silica interfaces. *Tribol. Lett.* **2014**, *56*, 481−490.
(58) Feigenbaum, A. Hydrogen bonding and retention on silica: A concept illustrated by TLC chromatography of nitrophenols. *J. Chem. Educ.* **1986**, *63*, 815.
(59) Yekeen, N.; Manan, M. A.; Idris, A. K.; Samin, A. M. Influence of surfactant and electrolyte concentrations on surfactant Adsorption and foaming characteristics. *J. Pet. Sci. Eng.* **2017**, *149*, 612−622.
(60) Yekeen, N.; Padmanabhan, E.; Idris, A. K.; Ibad, S. M. Surfactant adsorption behaviors onto shale from Malaysian formations: Influence of silicon dioxide nanoparticles, surfactant type, temperature, salinity and shale lithology. *J. Pet. Sci. Eng.* **2019**, *179*, 841−854.
(61) Malik, P. Dye removal from wastewater using activated carbon developed from sawdust: adsorption equilibrium and kinetics. *J. Hazard. Mater.* **2004**, *113*, 81−88.
(62) Özcan, A. S.; Erdem, B.; Özcan, A. Adsorption of Acid Blue 193 from aqueous solutions onto BTMA-bentonite. *Colloids Surf., A* **2005**, *266*, 73−81.
(63) Wang, C.-H.; Hwang, B. J. A general adsorption isotherm considering multi-layer adsorption and heterogeneity of adsorbent. *Chem. Eng. Sci.* **2000**, *55*, 4311−4321.
(64) Amin, M. T.; Alazba, A.; Shafiq, M. Nonspontaneous and multilayer adsorption of malachite green dye by Acacia nilotica waste with dominance of physisorption. *Water Sci. Technol.* **2017**, *76*, 1805−1815.
(65) Domínguez, A.; Fernández, A.; González, N.; Iglesias, E.; Montenegro, L. Determination of critical micelle concentration of some surfactants by three techniques. *J. Chem. Educ.* **1997**, *74*, 1227.
(66) Sánchez-Martín, M.; Dorado, M.; Del Hoyo, C.; Rodríguez-Cruz, M. Influence of clay mineral structure and surfactant nature on the adsorption capacity of surfactants by clays. *J. Hazard. Mater.* **2008**, *150*, 115−123.
(67) Musa, M. S. M.; Sulaiman, W. R. W.; Majid, Z. A.; Majid, Z. A.; Idris, A. K.; Rajaei, K. Henna extract as a potential sacrificial agent in reducing surfactant adsorption on kaolinite: The role of salinity. *J. King Saud Univ., Eng. Sci.* **2020**, *32*, 543−547.
(68) Belhaj, A. F.; Elraies, K. A.; Mahmood, S. M.; Zulkifli, N. N.; Akbari, S.; Hussien, O. S. The effect of surfactant concentration, salinity, temperature, and pH on surfactant adsorption for chemical enhanced oil recovery: a review. *J. Pet. Explor. Prod. Technol.* **2020**, *10*, 125−137.
(69) Saxena, N.; Kumar, A.; Mandal, A. Adsorption analysis of natural anionic surfactant for enhanced oil recovery: The role of mineralogy, salinity, alkalinity and nanoparticles. *J. Pet. Sci. Eng.* **2019**, *173*, 1264−1283.
(70) Agboola, M. O.; Bekun, F. V.; Joshua, U. Pathway to environmental sustainability: nexus between economic growth, energy consumption, CO_2 emission, oil rent and total natural resources rent in Saudi Arabia. *Resour. Policy* **2021**, *74*, No. 102380.

https://doi.org/10.1021/acsomega.3c00371
ACS Omega 2023, 8, 13118−13130